

HIA/Fuel System Development/Terminal Summary Report," NASA CR-111902, Dec. 1968.

⁴Masuya, G., and Wakamatsu, Y., "Calculation of Scramjet Performance," National Aerospace Lab., Japan, NAL TR-987, July 1988 (in Japanese).

⁵Waltrup, P. J., Anderson, G. Y., and Stull, F. D., "Supersonic Combustion Ramjet (Scramjet) Engine Development in the United States," *Proceedings of the 3rd International Symposium of Air Breathing Engines*, DGLR-Fachbuch No. 6, Munich, 1976, pp. 836-862.

⁶Sutton, G. P., and Ross, D. M., *Rocket Propulsion Elements*, 4th ed., Wiley, New York, 1976, pp. 82, 282, 318, and 329.

⁷Wakamatsu, Y., Kanmuri, A., and Toki, K., "Partial Bleed Expander Cycle for Low Thrust LOX/LH₂ Rocket Engine," National Aerospace Lab., Japan, NAL TR-837T, Sept. 1984.

⁸Anderson, G. Y., Eggers, J. M., Waltrup, P. J., and Orth, R. C., "Investigations of Step Fuel Injectors for an Integrated Modular Scramjet Engine," *Proceedings of the 13th JANNAF Combustion Meeting*, Chemical Propulsion Information Agency, Applied Physics Lab., Laurel, MD, Sept. 1976.

⁹Mayer, E., "Analysis of Convective Heat Transfer in Rocket Nozzles," *ARS Journal*, Vol. 31, No. 7, 1961, pp. 911-917.

Initial Development of a Pulsed Electrothermal Thruster

Rodney L. Burton* and Shih-Ying Wang†
GT-Devices, Inc., Alexandria, Virginia 22312

I. Introduction

THE pulsed electrothermal (PET) thruster¹⁻⁴ generates stagnation pressures of tens to hundreds of atmospheres by operating in a pulsed mode. For pulse widths of 10 μ s, the electrode and insulator surfaces stay below their melting points. The high operating pressure increases recombination in the nozzle to reduce frozen flow losses and exhaust gas temperatures.

The PET thruster system includes the thruster head, propellant injection system, capacitive energy storage system, power supply, and control system. The thruster head contains a cylindrical capillary discharge chamber with end electrodes, with water propellant injected along the centerline. The discharge heats the injected water to a high temperature and pressure during the pulse, creating a thrust impulse. The pulsed discharge breaks down at several hundred pulses/s to create average thrust. The 5-mm-inner-diam (ID) \times 56-mm-long cylindrical capillary insulator is made of prestressed silicon nitride or alumina⁴; smaller boron nitride insulators with 4- and 3.2-mm ID were also used.

The PET thruster head is water cooled, enabling thermal heat loss to be measured calorimetrically. The thruster is not sensitive to electrode polarity and is operated here with the propellant injected through the anode at the stagnation end. The grounded cathode is located at the sonic throat. The anode material is 0.15% alumina dispersion-strengthened copper or sintered tungsten alloy. The 400:1 contoured exhaust nozzle contains the tungsten alloy cathode as an insert.

Water propellant is continuously injected through a straight 75-100 μ m orifice with an L/D (length/diameter) of 1.5-5.0. At 200-400 pulses/s, the propellant only travels a few centimeters between pulses, so that injected, unevaporated liquid is

heated by two or three pulses. The water is injected either as a straight jet or atomized spray. A finite element thermal model is used to predict and avoid the onset of boiling at the orifice. A ceramic Macor thermal insulator prevents propellant boiling when operating near the ideal propellant flow. The water flow requirement for the PET thruster at 1500-s specific impulse is 6 mg/s/kW, giving 60 μ g/pulse at a typical pulse rate of 100 pulses/s/kW.

Spray injection is achieved through the technique of aerated liquid atomization.⁵ Helium gas is introduced upstream of the orifice, with the liquid and gas passing through the orifice as a mixture, producing a fine 20 μ m spray with a total spray angle of 15-20 deg. This approach uses a gas mass flow rate of 1-10% of the liquid mass flow rate. The resulting aerated liquid spray intersects the hot wall of the capillary where the droplets are partially evaporated, forming a vapor film that prevents further wall contact.

Based on studies of droplets exposed to gas dynamic shock waves,⁶ it is probable that axial vapor flow causes the drops to shatter on a time scale of a few μ s. The Weber number $\rho u^2 d / \sigma$ for 20 μ m drops is $We = 2 \times 10^3$ near the throat, greatly exceeding the critical Weber number $We \approx 5$. This shattering process is crucial to the coupling between the water and the discharge.⁷

The thruster is driven at 200-400 pulses/s by a 10 section, 10 μ F, 0.48 Ω pulse-forming network (PFN), using phenyl xylol ethane (PXE) dielectric capacitors with an estimated dielectric loss of 0.2 W at 5 kW. Predicted life is 10^9 - 10^{11} pulses. Demonstrated life here is $> 2 \times 10^7$ pulses with zero failures and 10^{11} pulses in a similar application, so that capacitor life is no longer considered an issue for the PET thruster. The PFN is designed to match the electrical resistance of the discharge and to prevent electrode or insulator surface melting during the pulse.⁴ The thruster is tested with axis vertical on a 1 m³ vacuum tank, with a tank pressure of 1 Torr.

II. Operational Tests

Tests were run at the several-kilowatt level to measure thruster operating parameters. Test experience with 56-mm-long ceramic insulators is summarized in Table 1, covering 26.6×10^6 total pulses.⁴

Insulator ablation was measured with dimensional gauge pins after each test. In no case was any erosion observed with Si₃N₄, Al₂O₃, or BN. Although the insulators experienced sputtering from the eroding electrodes, no dimensional change was detected and no change in electrical behavior was observed.

Electrode erosion was measured for thruster average power of 1.3-3.6 kW. Electrode mass loss for the PET thruster is plotted vs average thruster power in Fig. 1, covering a variety of anode geometries, anode materials, and arc conditions. Because plasma heat transfer does not cause electrode surface melting, the observed erosion is probably due to coulombic charge transfer. Experimental measurements for vacuum arcs show^{8,9} that charge transfer erosion decreases with pressure to 2-3 μ g/C at 500 Torr. Most of the present data fall below 10 μ g/C, much of it in the 2-4 μ g/C range, with cathode erosion

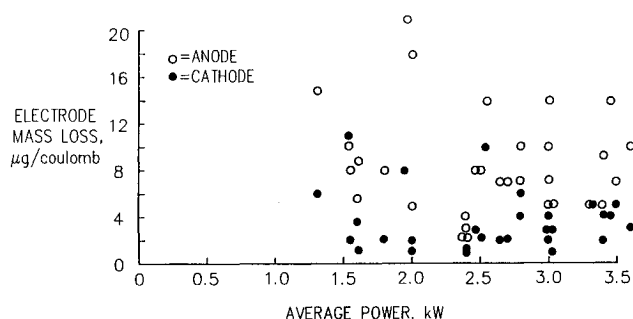


Fig. 1 Electrode mass loss, showing lower erosion for the cathode.

Presented as Paper 89-2265 at the AIAA 25th Joint Propulsion Conference, Monterey, CA, July 10-12, 1989; received Dec. 1, 1989; revision received May 5, 1990; accepted for publication June 7, 1990. Copyright © 1990 by the American Institute of Aeronautics and Astronautics, Inc. All rights reserved.

*Director, Space Applications; currently Associate Professor, Department of Aeronautical and Astronautical Engineering, University of Illinois, Urbana, IL. Member AIAA.

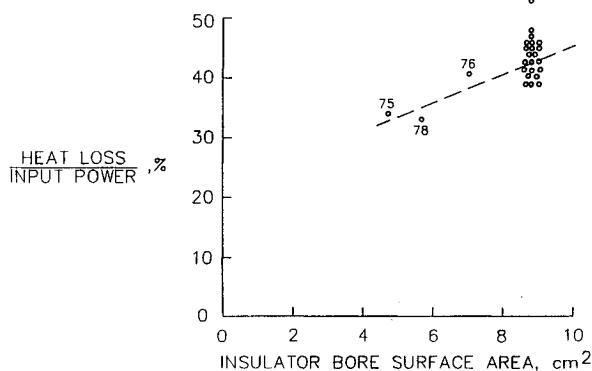
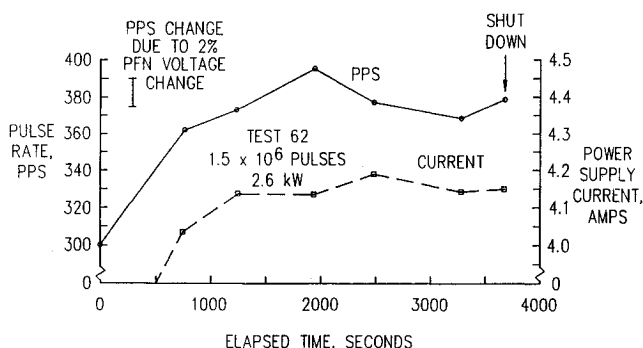
†Senior Scientist.

Table 1 Ceramic insulator tests

Insulator type	Si ₃ N ₄	Al ₂ O ₃	BN	BN	BN
Inner diameter, mm	5.0	5.0	5.0	4.0	3.2
Total tests	37	16	1	1	2
Pulses $\times 10^{-6}$	18.7	5.5	0.07	1.1	1.2

Table 2 Erosion at high propellant utilization, η_{pu}

	Test number			
	64	65	66	67
Total pulses $\times 10^{-6}$	0.7	1.0	2.0	1.1
Average power, kW	2.5	3.3	3.0	3.0
η_{pu}	0.67	0.66	0.95	0.91
Helium mass flow fraction	0.0	0.0	0.05	0.05
Si ₃ N ₄ erosion, $\mu\text{g}/\text{C}$	8.0	4.5	10.2	5.3
Cathode erosion, $\mu\text{g}/\text{C}$	3.4	4.5	2.4	1.2
Arc voltage, kV	1.2	1.5	1.5	1.5

**Fig. 2 Heat loss as a function of insulator surface area, determined calorimetrically.****Fig. 3 Variation in pulse rate and current for a 1-h test.**

considerably less than anode erosion. The lifetime of the electrodes can be extrapolated using the erosion data, resulting in 3×10^7 pulses per gram of electrode.

The ratio of ideal mass flow rate to the actual mass flow rate is called the propellant utilization efficiency η_{pu} . The ideal mass flow rate is calculated from the water enthalpy h at 100% of the actual pulse energy, based on discharge conditions: $\Delta m_{ideal} (\text{kg/pulse}) = E_{pulse}/h$. Propellant utilization < 1.0 reduces specific impulse, and so η_{pu} must be kept as high as possible. Erosion tests at high propellant utilization are summarized in Table 2.

Table 2 shows that injection with and without a 5% helium flow fraction has little effect on erosion or thruster voltage. All tests in Table 2 were performed without boiling the propellant or without an adverse effect on erosion.

The water cooling jacket on the PET thruster permits calorimetric measurement of the thermal efficiency. Data for the time-averaged cooling power on 28 tests are summarized in Fig. 2, which plots the thermal loss fraction as a function of bore surface area. Most of the data from Fig. 2 (open circles) are for a 5-mm-diam \times 56-mm-long ceramic insulator. Three data points (tests 75–78) show higher thermal efficiency associated with reduced surface area capillaries. The thruster thermal efficiency for tests 75 and 78 is about 0.66.

Performance degradation is measured in terms of the arc electrical properties. The variations in pulse rate and power supply current during a run of 1.5×10^6 pulses are shown in Fig. 3, where the error bar shows the expected range in pulse rate from a 2% variation in PFN voltage. Pulse rate variation is also a sensitive indicator of anode sputtering because a conductive coating on the insulator would reduce PFN voltage and raise pulse rate, which was not observed. Over this test period, degradation was probably $< 1\%$.

III. Analysis and Conclusions

For pulses that generate quasisteady conditions in the capillary, the nozzle enthalpy flux $\dot{m}h$ is equal to the plasma radiation intercepted by the propellant, thus giving: $\eta_{therm} = (Q_{rad})_{prop}/(I^2R)$. This expression emphasizes that arc radiation must be absorbed by the propellant, achieved either by coating the wall with an absorbing water layer or by spray injection of micron-size drops. For the latter case, the thermal efficiency is derived from the ratio of the wall surface area πDL to the droplet surface area A_{drop} . For the present 5-kW thruster at 250 pulses/s, $\eta_{therm} = 0.90$ for $0.1 \mu\text{m}$ drops.

Mechanisms for droplet shattering have been verified by us with high-speed photomicrographs⁷ showing shattering on a time scale of 15–30 μs after discharge initiation. The Weber number criterion predicts drop diameters of $< 0.1 \mu\text{m}$ near the nozzle exit. We also know that reducing capillary diameter raises the thermal efficiency, as shown in Fig. 2. This is consistent with the expected increase in pressure and flow velocity in the capillary, which in turn accelerates the process of drop breakup, evaporation, and radiation absorption.

Observed thruster erosion is consistent with erosion experience from vacuum arc discharges. The thruster is dependent on breakup of the injected liquid propellant for efficient operation, and so may benefit from longer discharge pulses than the 10 μs used here. Thruster erosion can also be reduced with higher voltage operation to reduce coulomb transfer.

Acknowledgments

This work was funded by the Strategic Defense Initiative Organization (SDIO) and NASA Lewis Research Center. The authors gratefully acknowledge the technical assistance of G. Jaafari in operating the PET thruster and designing some of the auxiliary systems, the design effort by D. Van Doren, the electronics support provided by T. Barrett, and the machining support by T. Golcher.

References

- Burton, R. L., Goldstein, S. A., Tidman, D. A., and Winsor, N. K., "Theory of the Pulsed Electrothermal Thruster," AIAA Paper 82-1952, Nov. 1982.
- Burton, R. L., Goldstein, S. A., Hilko, B. K., Tidman, D. A., and Winsor, N. K., "Investigation of a Pulsed Electrothermal Thruster System," NASA CR-174768, Oct. 1984.
- Burton, R. L., Fleisher, D., Goldstein, S. A., and Tidman, D. A., "Experiments on a Repetitively Pulsed Electrothermal Thruster," *Journal of Propulsion and Power*, Vol. 6, No. 2, 1990, pp. 139–145.
- Burton, R. L., and Wang, S. Y., "Ceramic Insulators for Pulsed

Electrothermal Devices," GT-Devices, Inc., Alexandria, VA, Final Rept. 89-5, May 1989.

⁵Lefebvre, A. H., Wang, X. F., and Martin, C. A., "Spray Characteristics of Aerated-Liquid Pressure Atomizers," *Journal of Propulsion and Power*, Vol. 4, No. 4, 1988, pp. 293-298.

⁶Wierzbna, A., and Takayama, K., "Experimental Investigation of the Aerodynamic Breakup of Liquid Drops," *AIAA Journal*, Vol. 26, No. 11, 1988, pp. 1329-1335.

⁷Burton, R. L., and Hilko, B. K., "Heating of a Liquid/Vapor Mixture by a Pulsed Electric Discharge," GT-Devices, Inc., Alexan-

dria, VA, Tech. Rept. GTD 88-8, July 1988.

⁸Kimblin, C. W., "Cathode Spot Erosion and Ionization Phenomena in the Transition from Vacuum to Atmospheric Pressure Arcs," *Journal of Applied Physics*, Vol. 45, No. 12, 1974, pp. 5235-5244.

⁹Meunier, J.-L., and Drouet, M. G., "Experimental Study of the Effects of Gas Pressure on Arc Cathode Erosion and Redeposition in He, Ar, and SF₆ from Vacuum to Atmospheric Pressure," *IEEE Transactions on Plasma Science*, Vol. PS-15, No. 5, 1987, pp. 515-519.

*Recommended Reading from the AIAA
Progress in Astronautics and Aeronautics Series . . .*



Thermal Design of Aeroassisted Orbital Transfer Vehicles

H. F. Nelson, editor

Underscoring the importance of sound thermophysical knowledge in spacecraft design, this volume emphasizes effective use of numerical analysis and presents recent advances and current thinking about the design of aeroassisted orbital transfer vehicles (AOTVs). Its 22 chapters cover flow field analysis, trajectories (including impact of atmospheric uncertainties and viscous interaction effects), thermal protection, and surface effects such as temperature-dependent reaction rate expressions for oxygen recombination; surface-ship equations for low-Reynolds-number multicomponent air flow, rate chemistry in flight regimes, and noncatalytic surfaces for metallic heat shields.

TO ORDER: Write, Phone or FAX:

American Institute of Aeronautics and Astronautics,
c/o TASC0, 9 Jay Gould Ct., P.O. Box 753, Waldorf, MD 20604
Phone (301) 645-5643, Dept. 415 • FAX (301) 843-0159

Sales Tax: CA residents, 7%; DC, 6%. For shipping and handling add \$4.75 for 1-4 books (call for rates for higher quantities). Orders under \$50.00 must be prepaid. Foreign orders must be prepaid. Please allow 4 weeks for delivery. Prices are subject to change without notice. Returns will be accepted within 15 days.

1985 566 pp., illus. Hardback
ISBN 0-915928-94-9
AIAA Members \$54.95
Nonmembers \$81.95
Order Number V-96